ISIJ International, Vol. 54 (2014), No. 4, pp. 827–835

Interfacial Reaction between Al_2O_3–SiO_2–C Refractory and Al/Ti-Killed Steels

Young Seok LEE,[1] Sung-Mo JUNG[2]* and Dong-Joon MIN[3]

1) Technical Research Laboratories, POSCO, Pohang, 790-785 Korea.
2) Graduate Institute of Ferrous Technology, POSTECH, Pohang, 790-784 Korea.
3) Department of Metallurgical System Engineering, Yonsei University, Seoul, 120-749 Korea.

(*Received on March 1, 2013; accepted on December 5, 2013*)

In the current investigation, the thin film method was employed to clarify the formation mechanism of the oxide layers at the interface between the Al_2O_3–SiO_2–C refractory and liquid Fe. A reacted layer was formed in such a way that initially FeO-enriched liquid layers are widely distributed on the Fe surface and FeO and SiO_2 in the liquid layer are reduced by Al in liquid Fe to develop solid Al_2O_3-enriched layer of inclusions. Some inclusions in liquid Fe might be produced by the remaining oxygen in Ar gas being supplied through the nozzle to prevent the adherence of inclusions onto it. The oxide layers at the interface estimated by thermodynamic calculation are in good accordance with the experimental results of the reaction between Al_2O_3–SiO_2–C refractory and Al-killed/Al-Ti-killed steels previously reported.

KEY WORDS: nozzle clogging; Al_2O_3–SiO_2–C refractory; Al-killed steel; Al/Ti-killed steel; interfacial reaction; inclusion.

1. Introduction

Production of ultra clean steel has led a growing emphasis on the proper control of nonmetallic inclusions in steels. Refractory materials have been indicated as one of the major sources of non-metallic inclusions in the molten steel during ladle metallurgy.[1–5] Al_2O_3 agglomeration onto a tundish nozzle has been a serious problem with the continuous casting process of steel. Nozzle clogging by agglomerated Al_2O_3 lead to a non-uniform flow of molten steel in the mold and to the defects in products from large Al_2O_3 inclusions separated from the clogged nozzle.[6] Several investigations on the clogging mechanism and its prevention have been reported.[6–11] In particular, the interfacial reactions between the nozzle and molten steel have been receiving extensive attention since the formation and growth of inclusions generated by the interfacial reactions are ascribed to the nozzle clogging. This indicates that the reaction products between the constituting oxides in nozzles and deoxidation elements in molten steel are accumulated at the interface. There have been numerous studies about nozzle clogging in Al-killed and Al/Ti-killed steels, which are supported by the consistent observation that the accumulated oxide layers on the nozzle surface are similar to the nozzle materials in terms of the constituting elements.

Sasai *et al.*[12] clarified the formation mechanism of reacted layer in Al-killed and Ti-killed steels. They reported that SiO_2 in refractory was reduced by carbon to produce SiO and CO gases and that SiO_2 in refractory reacted with Al or Ti in molten Fe to generate Al_2O_3 or Ti_3O_5 inclusions. Kaneko *et al.*[13] also reported that Al or Ti in molten Fe directly reduced SiO_2 in refractory. In most cases, it is well known that a reticulate layer is formed on the surface of a refractory and another tight layer of alumina cluster is added onto it. In the case of Al-killed steel, it is difficult to make a difference between the reticulate and tight layers since Al_2O_3 is the major component in both layers. However, although the Al–Ti–O layer on the surface of a refractory and the layer of Al_2O_3 cluster were easily identified in the case of Al/Ti-killed ultralow carbon steel, it is not easy to separate both the layers from a viewpoint of nozzle clogging. Therefore, it is required to clarify the effect of interfacial reaction between actual nozzle and molten steel by employing new experimental technique.

It is required to investigate the formation and behavior of inclusions at the interface adjacent to the refractory since it is difficult to clearly identify the interface in the conventional experimental methods employing the reaction of refractory with molten steel. Therefore, in the present study, a thin film method was employed to clarify the effect of interfacial reaction between Al_2O_3–SiO_2–C refractory and liquid Fe on the formation and evolution of inclusions at the interface.

2. Experimental

2.1. Materials Preparation

According to Dekkers *et al.*,[14,15] the formation of metastable secondary particles was unavoidable in the course of sampling regardless of the sampler used. It is believed that this is the most ambiguous factor affecting the analysis of the morphology and size of inclusions adjacent to the inter-

* Corresponding author: E-mail: smjung@postech.ac.kr
DOI: http://dx.doi.org/10.2355/isijinternational.54.827

face between the refractory and molten iron. Therefore, the thin film method developed in the current study would facilitate the clear explanation of the effects of supersaturation degree, reaction time and surface roughness of the substrate on the morphology and size distribution of alumina inclusions formed at the iron/refractory interface. The validity of the method suggested in the current research was evaluated by analyzing the morphology and composition of inclusions using SEM and EPMA. That is, it was confirmed that the current method could sufficiently be reasonable for simulating interfacial reactions between the substrate and liquid iron.

As shown in **Fig. 1**(a), the lower supporting material of the sample assembly is the alumina single crystal substrate whose top side was coated with pure aluminum (>99.999%) of variable thickness to control the Al content in liquid Fe using the general sputtering method (70 W, Ar 5 mL/min). And a pure Fe foil of 100 μm thickness (>99.99%, 15×15 mm^2) was placed on top of the coated side in a way that the aluminum on the substrate can diffuse through the layer of liquid Fe. Initial compositions of the Fe foil used in the current experiment are listed in **Table 1**. In case pure Al (>99.999%) of about 1 μm thickness was coated on the substrate, the Al content in liquid iron was estimated to be about 0.06 mass% under the assumption that all the Al dissolved into the pure Fe foil. As the upper substrate, Al_2O_3–SiO_2–C refractory was used. **Table 2** shows the chemical composition of Al_2O_3–SiO_2–C refractory before and after decarburization. The Al_2O_3–SiO_2–C refractory was sufficiently decarburized by the preheating. The surface roughness of the refractory was not available since the measured values were much beyond the upper limit of measuring capacity. Then the sample assembly was wrapped by ash-less paper, dipped into Al_2O_3 powder in a graphite crucible, and a cylindrical tungsten weight was placed on top of Al_2O_3 powder.

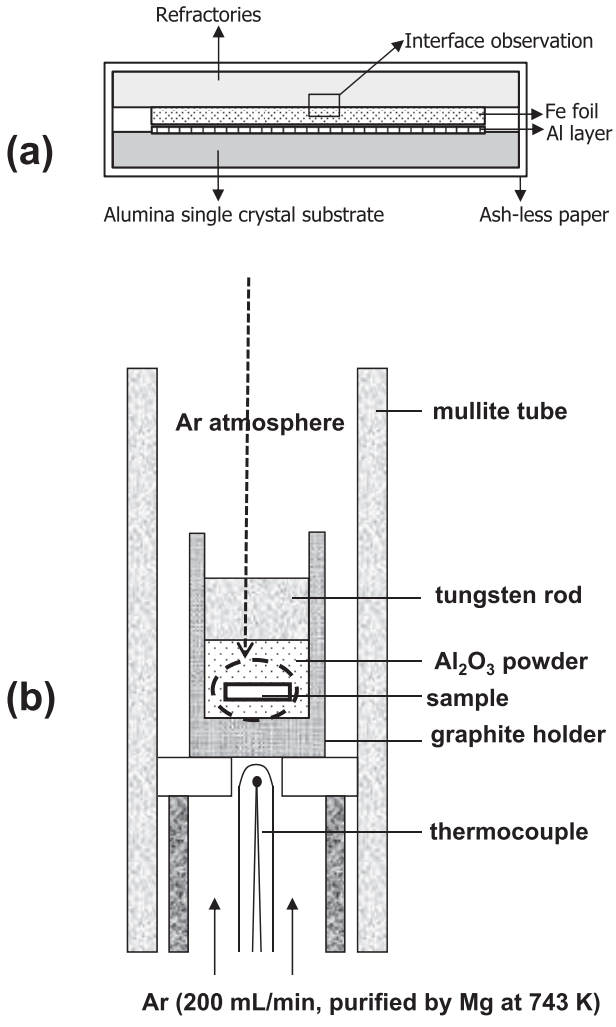

Fig. 1. Schematic diagram of (a) sample assembly and (b) experimental setup.

2.2. Experimental Procedure

A vertical electrical resistance furnace was employed as shown in Fig. 1(b). The temperature was automatically controlled within ±2 K using an R-type thermocouple (Pt-13%Rh/Pt) and a PID controller. The sample assembly was put into the furnace purged with Ar (6N purity) gas preliminarily purified by passing through Mg chips at 723 K to remove residual oxygen. After equilibrating for 3 hours, the graphite crucible containing the sample assembly was quickly withdrawn out of the furnace and quenched with water. The refractory/Fe interface containing inclusions was observed using FE-SEM (Hitachi, S-4200). The concentration of oxygen and nitrogen in the iron sample was analyzed by the combustion method using LECO^{TM} TC-300.

3. Results and Discussion

3.1. Effect of Refractory Materials on the Interfacial Reaction between Al_2O_3–SiO_2–C and Liquid Fe

Figure 2 shows the surface image of Fe sample obtained after raw Al_2O_3–SiO_2–C refractory reacted with liquid Fe containing 0.06 mass% of Al for 3 hours at 1 823 K. It was observed that the reacted layer of approximately 100 μm exists between the refractory and Fe. Due to the limitation in analyzing the compositional change of the constituents in the reacted layer by macroscopic analysis, the reacted layer was further magnified and analyzed by SEM/EDS. According to SEM/EDS analysis of the reacted layer, its averaged composition was analyzed to be 1.5%FeO-3.7%SiO_2-94.8%Al_2O_3. When moving from the refractory side to Fe, the proportion of Al_2O_3 gradually decreased, which is similar to the results of the reacted layer formed between Al_2O_3–C refractory and liquid Fe.[16] In order to observe the

Table 1. Initial compositions of Fe foil used in the present study (mass%).

Fe	C	N	S	Mn	Si	Mg	Al	O
balance	0.009	0.003	0.0002	trace	0.0009	trace	trace	0.017

Table 2. Chemical compositions of Al_2O_3–SiO_2–C refractory before and after decarburization (mass%).

	Before decarburization	After decarburization
Al_2O_3	38.2 – 47.6	55.4
SiO_2	29.6 – 38.9	43.5
Fe_2O_3	0.3 – 0.9	0.41
Fixed C + SiC	18.4 – 35.2	0.11
Na_2O		0.37
MgO		0.20

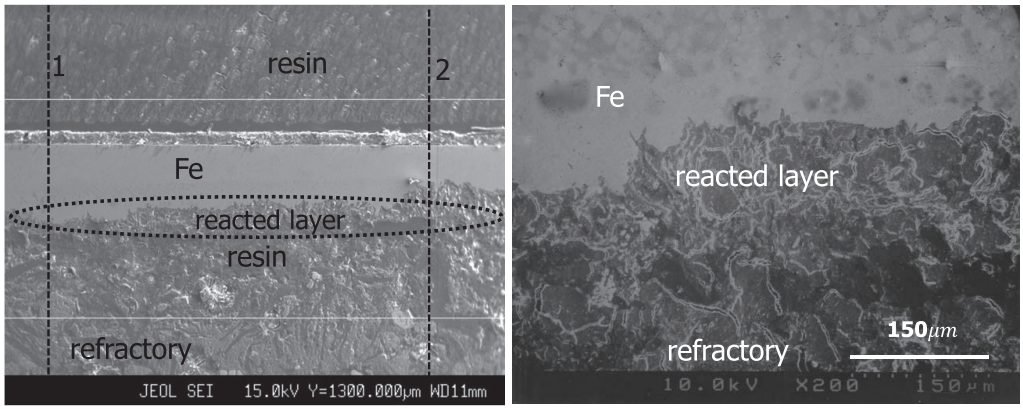

(a) Refractory/reacted layer/Fe (b) Reacted layer

Fig. 2. SEM image of the reacted layer formed by the reaction between raw Al_2O_3–SiO_2–C refractory and liquid Fe.

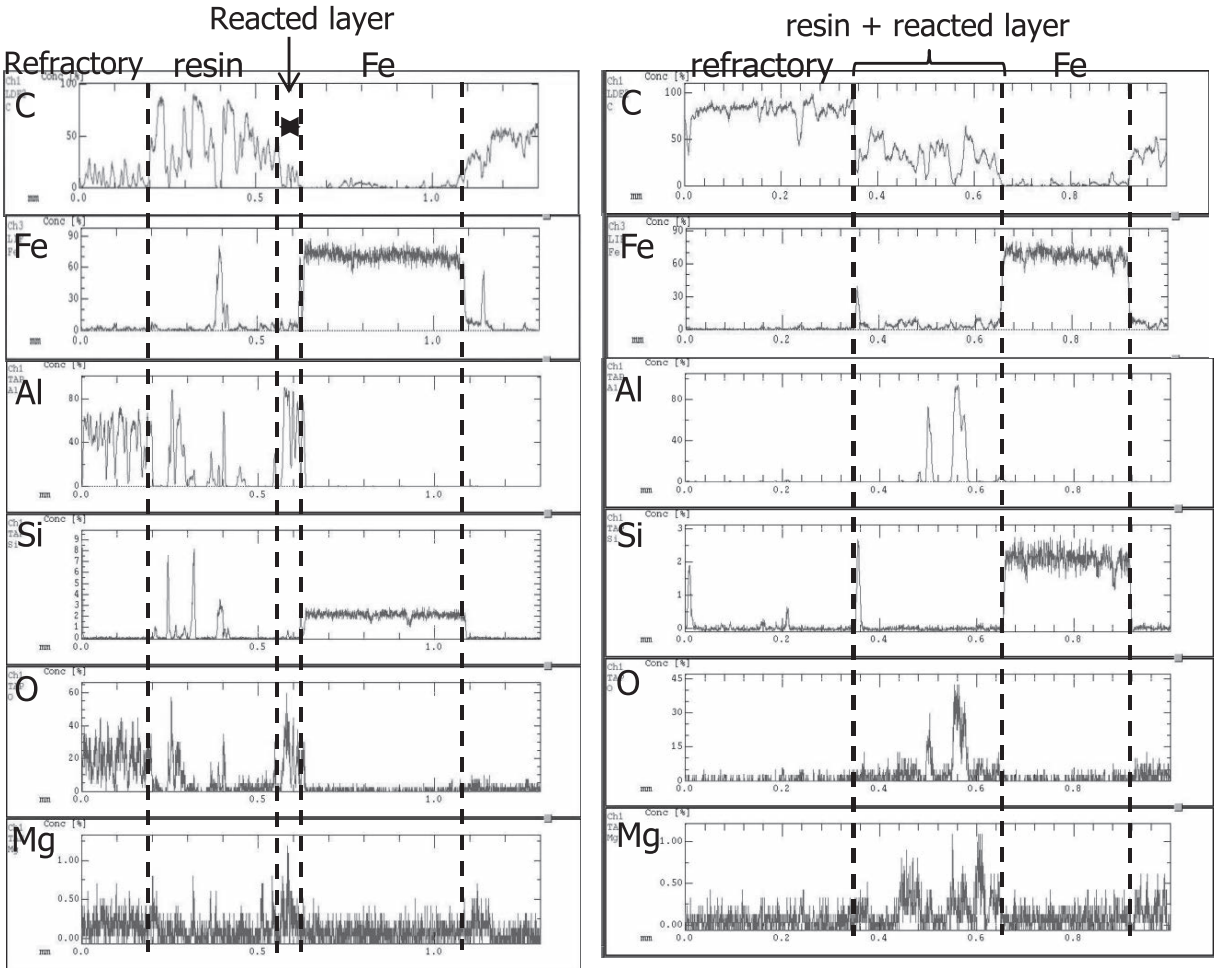

(a) Across line 1 (b) Across line 2

Fig. 3. Line mapping results of interfacial area after reaction between the refractory before preheating and Al-killed steel.

compositional change of the constituents, EPMA line mapping was carried out across the interface along the lines 1 and 2 in Fig. 2 and the results are shown in **Fig. 3**. It is clear that the concentrations of carbon and Si increased in Fe after the reaction. It is believed that some inclusions comprising FeO–SiO_2–Al_2O_3–MgO exist in the reacted layer, which has been solidified after melting. It is expected that the increase of carbon in liquid Fe is ascribed to the dissolution of carbon in the refractory or to the introduction of CO gas formed by the reaction between SiO_2 and carbon in the refractory. The increase of Si in liquid Fe is due to the reaction between Al in liquid Fe and SiO gas formed by the reaction between SiO_2 exposed to the surface of the refractory and carbon as explained by Eqs. (1) and (2).

$$SiO_2(s) + C(s) = SiO(g) + CO(g) \quad \text{..... (1)}$$

$$3SiO(g) + 2\underline{Al} = 3\underline{Si} + Al_2O_3(s) \quad \text{..... (2)}$$

$$3CO(g) + 2\underline{Al} = 3\underline{C} + Al_2O_3(s) \quad \text{..... (3)}$$

Figure 4(a) shows the interface formed by the reaction between the preheated Al_2O_3–SiO_2–C refractory and liquid Fe containing 0.1 mass% of Al for 3 hours at 1 823 K. As can be expected by the Reactions (1) to (3), the lower amount of Al_2O_3 inclusions can be formed in case less SiO(g) and CO(g) will be generated by the decreased activity of carbon in the preheated refractory. Thus, liquid Fe containing slightly larger amount of Al was used in a way that similar amount of Al_2O_3 inclusions would be formed in liquid Fe by driving the forward reactions of Eqs. (2) and (3). It was observed that the reacted layer of about 50 to 170 μm exists between the refractory and Fe. This reacted layer is separated from the coarse refractory and looks denser than the refractory. As previously performed, the reacted layer

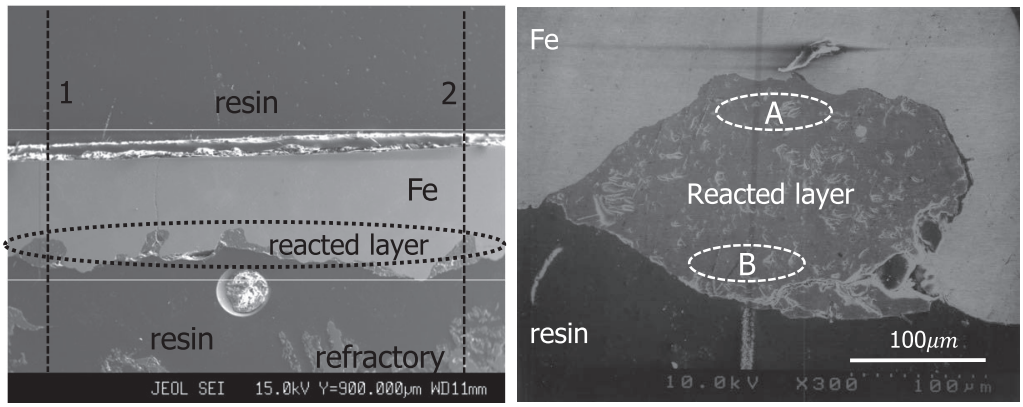

(a) Refractory/reacted layer/Fe (b) Reacted layer

Fig. 4. SEM image of the reacted layer formed by the reaction between preheated Al_2O_3–SiO_2–C refractory and liquid Fe.

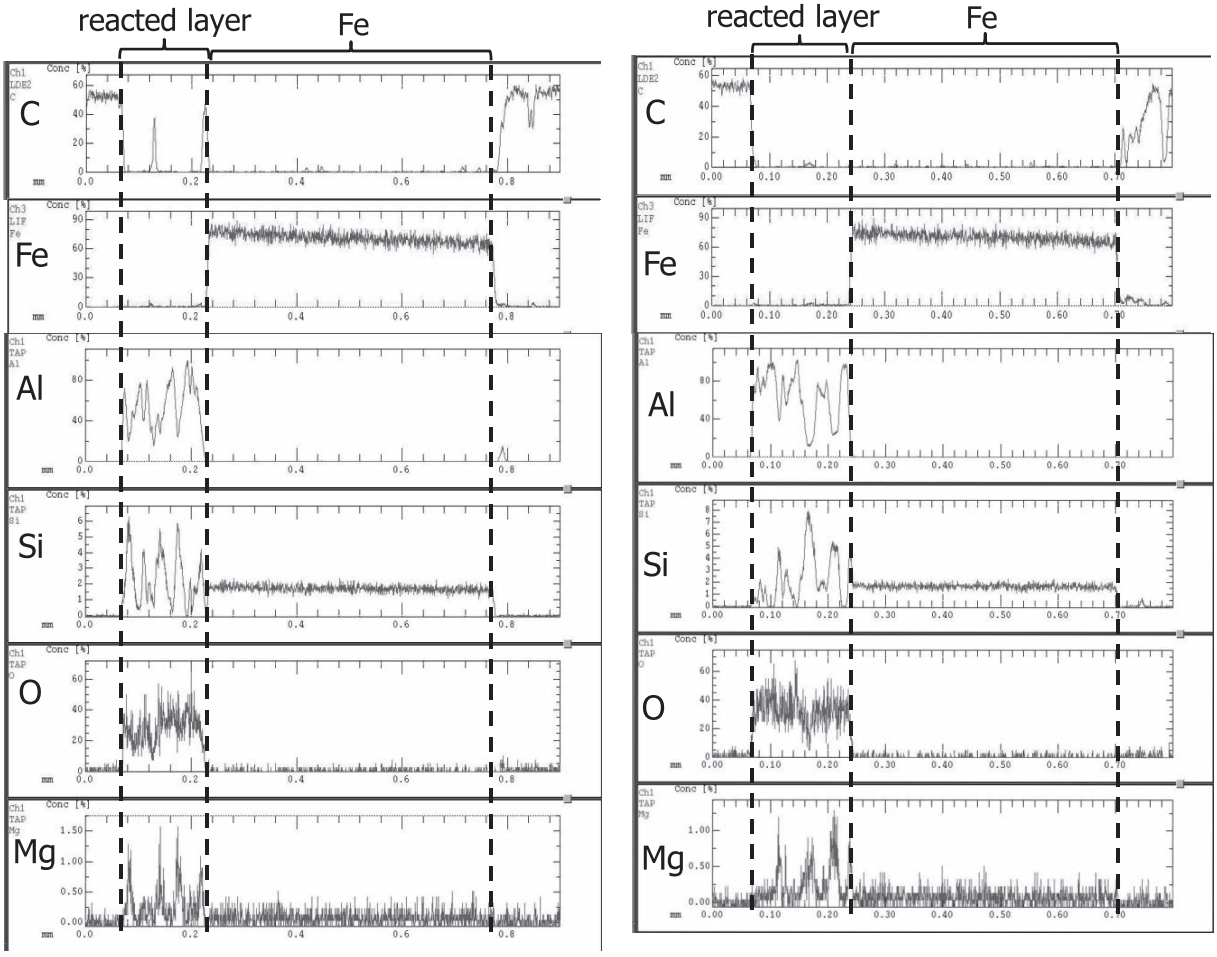

(a) Across line 1 (b) Across line 2

Fig. 5. Line mapping results of interfacial area developed by the interfacial reaction between the preheated refractory and liquid Fe.

was further magnified as shown in Fig. 4(b) and analyzed by SEM/EDS. The average composition of zone A located adjacent to Fe was 5.4%FeO-50.8%SiO_2-43.8%Al_2O_3. Zone B located closer to the refractory was analyzed to be 0.6%FeO-58.8%SiO_2-40.6%Al_2O_3. That is, when moving from the refractory side to Fe, the proportion of SiO_2 gradually decreased while the contents of FeO and Al_2O_3 increased. Although the compositions of A and B are in solid state according to FeO–SiO_2–Al_2O_3 phase diagram at 1 823 K,[17] the growth of reacted layer cannot be explained by the transfer of oxygen in terms of SiO(g) and CO(g) produced by the reaction between SiO_2 and carbon in the refractory since the refractory contains almost no carbon. Therefore, the current results are ascribed to the involvement of oxygen as a surface active element in the reaction, which is in good agreement with the previously reported ones.[18,19] That is, FeO-enriched inclusions (FeO–SiO_2–Al_2O_3) observed in Al-killed Fe are gradually reduced to Al_2O_3 by Al dross initially injected. It is believed that the reacted layer can be formed in such a way that initially FeO-enriched liquid layer of inclusions are widely distributed on Fe surface. Then, FeO and SiO_2 in the liquid layer are reduced by Al in liquid Fe, which ends up with the development of solid Al_2O_3-enriched layer of inclusions with increasing the number of inclusions. Then the inclusions might be pushed back toward the refractory as Al_2O_3 content in the inclusion increases.

As shown in **Fig. 5**, EPMA line mapping was carried out across the interface along the lines 1 and 2 in Fig. 4(a) to observe the compositional change of the constituents. The increase of carbon content in Fe layer was remarkably not observed compared with the case of the raw refractory. In general, the carbon in liquid Fe is normally identified due to the reaction between carbon-containing refractory and Fe. This is ascribed to the low carbon content remaining in the preheated refractory with other oxide constituents unchanged. Therefore, it is believed that the supply of oxygen toward the surface of liquid Fe is not available by the reaction between SiO_2 and carbon in the refractory as previously mentioned. On the other hand, it is believed that the increase of Si in Fe is ascribed to the reduction of SiO_2 exposed to the refractory surface after decarburization directly by Al in liquid Fe as explained by Eq. (4). This can be supported by the EPMA mapping result that the reacted layer shows very high Al_2O_3 content and slight amount of FeO, SiO_2 and MgO. After all, it is believed that the increase of Si in Fe is ascribed to the non-uniformity of the preheated refractory.

$$3SiO_2(s) + 4\underline{Al} = 3\underline{Si} + 2Al_2O_3(s) \quad \text{..... (4)}$$

3.2. Interfacial Reaction between Non-uniform SiO_2 in Refractory and Liquid Fe

In case the raw refractory contains carbon, the reaction between the SiO(g) or CO(g) supplied from the refractory and Al in liquid Fe could take place to produce Al_2O_3 inclusions as represented by Eqs. (2) and (3). However, in the case of decarburized refractory, the reaction between SiO_2 exposed to the refractory surface and Al in liquid Fe could occur to generate Al_2O_3 inclusions and to increase Si level in Fe as indicated by Eq. (4). From the remaining FeO in the reacted layer, the reaction between Al in Fe and FeO–SiO_2–Al_2O_3 inclusion resulted from the interaction between FeO and refractory could proceed.

Before the reaction between SiO_2 exposed in the refractory and liquid Fe is examined, the reaction between pure quartz and liquid Fe containing no Al was considered. **Figure 6** shows the surface of Fe reacted with quartz for 3 hours at 1 823 K. It is clear that no inclusions were observed on Fe surface. According to EDS analysis, only small amount of FeO and Fe was detected. In order to thermodynamically examine the decomposition of pure SiO_2, [%Si] content in liquid Fe was estimated based on the initial [%O] in Fe listed in Table 1.

$$SiO_2(s) = \underline{Si} + 2\underline{O} \quad \text{..... (5)}$$

$$\log K \left(= \log a_{Si} \cdot a_O^{\,2}\right) = -30\,110/T + 11.4^{20)} \quad \text{..... (6)}$$

Based on Eq. (6), about 0.026 mass% of Si would be in equilibrium with 0.017 mass% of O for the pure SiO_2. Ther-

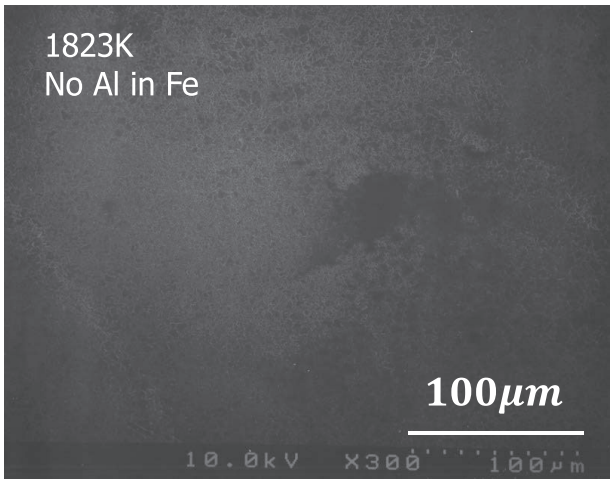

Fig. 6. SEM image on Fe surface between quartz and liquid Fe.

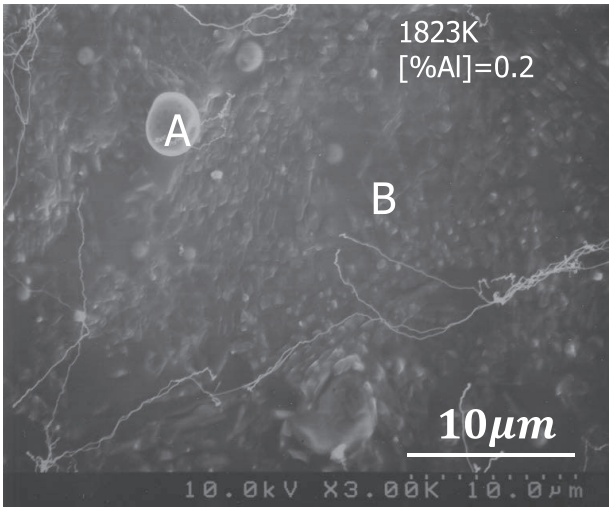

A: 31.6%FeO-62.4% SiO_2-6.0%Al_2O_3
(Sphere type)

B: 1.38%FeO-51.5%SiO_2-47.2%Al_2O_3
(Cluster: coral type)

Fig. 7. SEM image on quartz surface between quartz and liquid Fe.

modynamically it is likely that pure SiO_2 directly decomposes into Si and O in liquid Fe, which results in the dissolution of some Si in Fe for the initial O content of 0.017 mass%. Therefore, it was confirmed that pure quartz might decompose into Si and O in liquid Fe without forming any kind of inclusion. **Figure 7** shows the surface of quartz reacted with liquid Fe containing 0.2 mass% of Al. Spherical particles and coral-shaped cluster of inclusions were observed. According to EDS analysis, the composition of spherical particle A in Fig. 7 was 31.6%FeO-62.4%SiO_2-6.0%Al_2O_3 and that of part B was 1.38%FeO-51.5%SiO_2-47.2%Al_2O_3. On the other hand, **Fig. 8** shows the surface of Fe reacted with quartz. According to EDS analysis, the composition of coral-shaped cluster of inclusions was 4.0%FeO-29.5%SiO_2-66.5%Al_2O_3. Therefore, it can be understood that FeO and SiO_2 can be reduced by Al in liquid Fe.

Figure 9 shows the surface of Al_2O_3 single crystal facing liquid Fe. Spherical particles and coral-shaped cluster of inclusions were observed. According to EDS analysis, the composition of spherical particle A in Fig. 9 was 24.1%FeO-67.2%SiO_2-8.7%Al_2O_3 and that of part B was 20.3%SiO_2-79.7%Al_2O_3. It is understood that the Si supplied by the interfacial reaction between non-uniform SiO_2 in the refractory and liquid Fe would have the opposite diffusion path to Al and that Al and Si have counter-diffusion each other. Therefore, the SiO_2 exposed by non-uniformity of refractory can be reacted with Al in liquid Fe, which results in forming solid Al_2O_3-enriched inclusions as represented by Eq. (4). After all, it is believed that this process might cause the serious nozzle clogging.

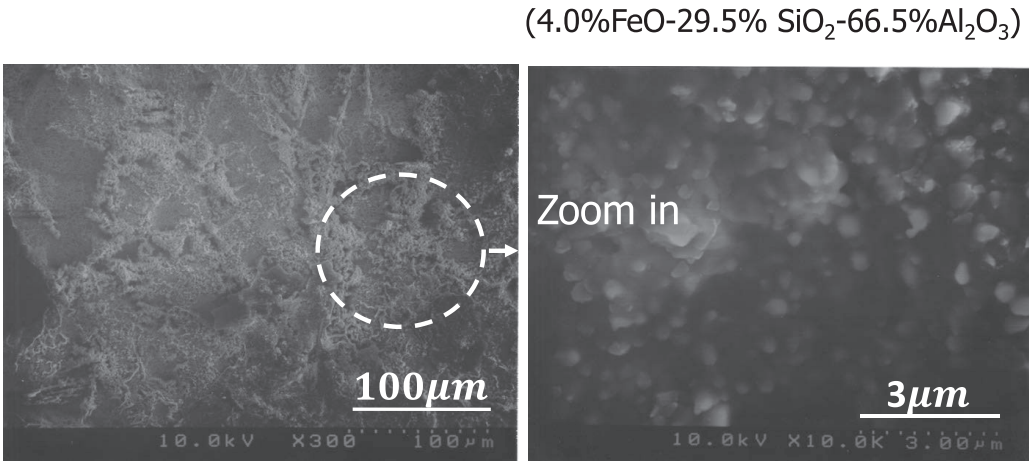

Fig. 8. SEM image on Fe surface between quartz and liquid Fe.

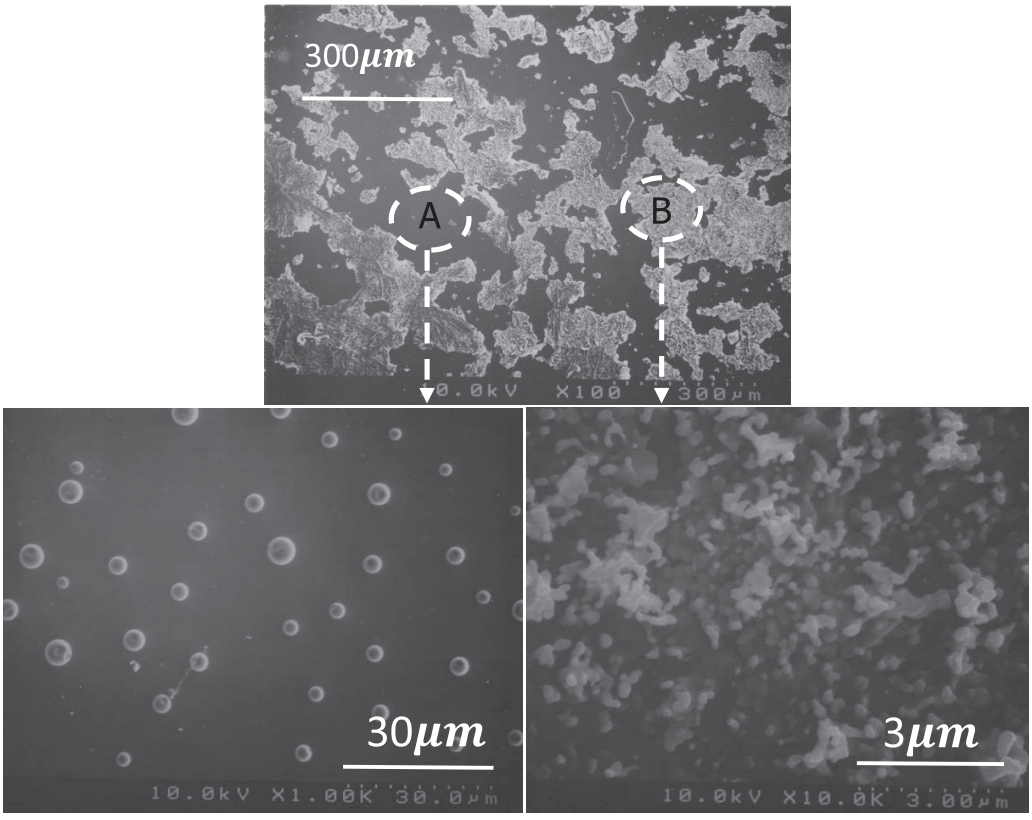

Fig. 9. SEM image on the surface of Al_2O_3 single crystal substrate between Al_2O_3 and liquid Fe.

3.3. Interfacial Reaction Affected by the Formation of FeO on the Surface of Liquid Fe

The surface activity of oxygen, J_O is defined as the slope of the surface tension, σ vs X_O at infinite dilution:

$$J_O = -\left(\frac{\partial\sigma}{\partial X_O}\right)_{X_{Fe}\to 1} = \left(RT\Gamma_{Fe}^{\circ}\right)\nu_O^{\infty} \quad \text{..... (7)}$$

where Γ_{Fe}° is the adsorption coefficient of almost pure Fe and ν_O^{∞} is adsorption coefficient of O at infinite dilution. It is well known that those values can be very high and that the concentration of a surface-active species at an interface is often several thousand times higher than that in the bulk.[21] At 1 823 K, J_O was calculated to be about 1 030. This means that the concentration of oxygen at Fe surface is about 1 030 times higher than that in the bulk. As shown in **Fig. 10**, the activity of O on Fe surface can be increased to Point B (3 090 ppm O) from Point A where Al of 400 ppm and oxygen of 3 ppm are in equilibrium. This can induce the super-saturation corresponding to the difference between Points B and A. Therefore, it is believed that 170 ppm oxygen used in the current experiment has sufficient driving force to form FeO on the Fe surface. The activated tendency of oxygen on Fe surface might result in the unstable state on the surface of liquid Fe and means that Fe easily oxidizes to FeO on the Fe surface thermodynamically. According to Ono-Nakazato *et al.*,[22] the Al content on Fe surface is about 1.7 times larger than that in the bulk of Fe as a deoxidizing element. Therefore, it is believed that the formation of Al_2O_3 at the interface between the refractory and liquid Fe will be promoted. Although Fe initially contains about 170 ppm of oxygen, the current oxygen content is almost equal to that in actual molten steel considering that the molten steel contains about 1 000 ppm of Al and that the reaction time is about 3 hours. In comparison with actual casting conditions, the FeO layer can react with the refractory materials to form melt layer since the FeO layer on the surface is formed in the initial period of casting. Then, the melt reacts with Al in liquid Fe, which is followed by the gradual growth of the reacted layer. This reacted layer is gradually enriched in Al_2O_3, which results in the increase of melting point. Then the solid inclusions would move toward the refractory wall by interfacial tension between the refractory and liquid Fe. Therefore, it is understood that the layer of inclusions formed at the interface consists of the layer similar to the refractory materials and Al_2O_3 layer. The Al_2O_3 layer is successively produced by the reaction between Al in liquid Fe and liquid FeO–SiO_2–Al_2O_3 or SiO(g)/CO(g) supplied from the refractory containing carbon. This indicates that the coral-shaped Al_2O_3 layer is more outstanding than dendrite-shaped one. After all, the liquid layer of inclusions will play a role in attaching the deoxidation inclusions to the refractory wall.

3.4. Effect of the Remaining Oxygen in Supplied Ar Gas on the Formation of Inclusions

It can be considered that the inclusions in liquid Fe can be formed due to the oxygen included in Ar gas which is supplied through nozzle to prevent the adherence of inclusions onto it. **Figure 11** shows the analyzed content of oxygen in liquid Fe through which Ar was blown for 3 hours when the initial content of oxygen was 0.05 mass%. Two kinds of Ar gases were used. The first Ar gas (99.999% purity) was sufficiently deoxidized by passing through Mg turnings preliminarily and the second Ar gas was directly supplied without deoxidation. In the chemical analysis, the specimen surface was slightly dissolved into HCl(1 + 10) for 30 min in such a way that FeO on the surface could not affect the analysis of oxygen in the bulk of Fe. The activity of Fe_tO in Fig. 11 was evaluated according to the following equilibrium between liquid Fe and dissolved oxygen:

$$\mathrm{Fe}(l) + \underline{\mathrm{O}} = \mathrm{Fe_tO}(l) \quad \text{..... (8)}$$

$$\Delta G^{\circ} = -138\,910 + 57.00T\,(\mathrm{J/mol})^{23)} \quad \text{..... (9)}$$

$$K = \exp(-\Delta G^{\circ}/RT) = \frac{a_{Fe_tO}}{a_{Fe}(\approx 1)\cdot a_O} \quad \text{..... (10)}$$

where the standard state of oxygen is the infinitely dilute solution of Fe–O and the activities of Fe and Fe_tO are with respect to pure liquids. Then the partial pressure of oxygen was estimated from the dissolved oxygen in liquid Fe:

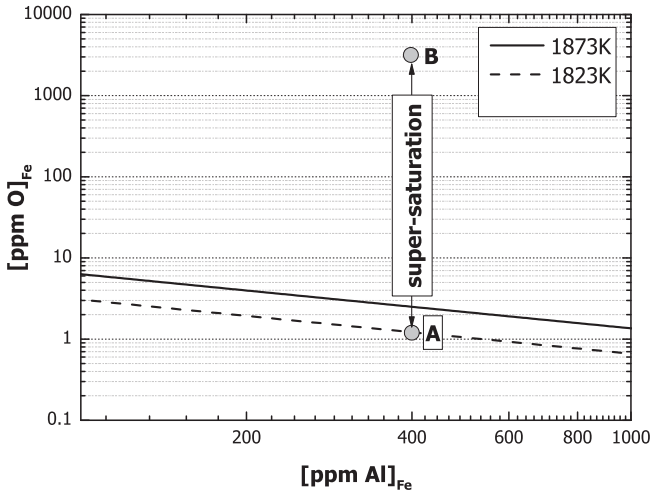

Fig. 10. Al–O equilibrium in liquid Fe.[20]

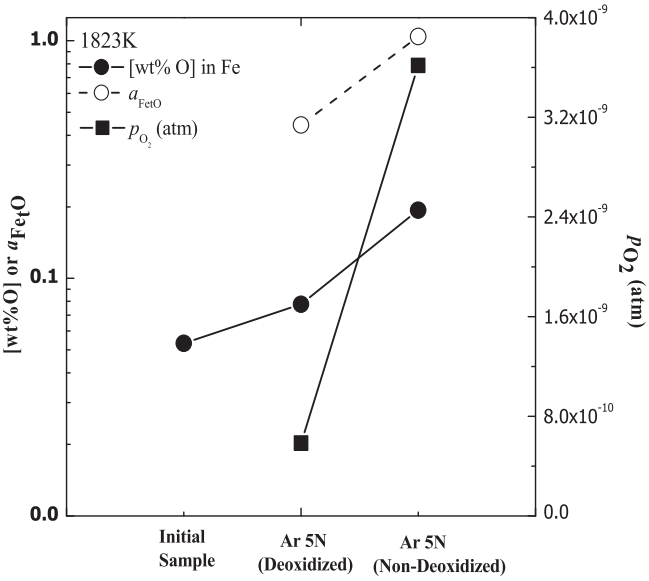

Fig. 11. Effect of oxygen partial pressure on the oxygen in liquid Fe.

$$\underline{O} = \frac{1}{2} O_2(g) \quad \text{..... (11)}$$

$$\Delta G^\circ = 117\,150 + 3.32T(\text{J/mol})^{23)} \quad \text{..... (12)}$$

From Fig. 11, it is clear that even Ar gas of 99.999% purity can cause to form inclusions due to the remaining oxygen in Ar gas. Although the blowing of Ar into nozzle for preventing the clogging can help separate the layer of inclusions attached to the wall of nozzle, it can increase the oxygen content around the bubbles due to the oxygen in Ar gas. Then the increased O content in bubbles might react with the deoxidizing elements, which end up with the formation of inclusions in liquid Fe. Accordingly, it is of great importance to use Ar gas fully deoxidized to prevent the formation of nozzle clogging.

3.5. Thermodynamic Prediction of Interfacial Oxide Layers

Based on the formation of inclusions at the interface between the refractory and liquid Fe, thermodynamic calculation was carried out to predict the characteristics of reacted layer and the thickness of inclusion layer. The calculation was performed using thermodynamic calculation software, FactSage5.2. Fundamental assumptions and procedure for the calculation are as follows: (1) The composition in the inner part of the refractory remains unchanged since only the surface is decarburized in actual process. (2) The initial reaction occurred among the liquid Fe, the produced gases from refractory materials and the remaining constituents in the refractory of 1 mole. (3) Solid inclusions resulted from the reaction stick to the refractory and that they are not involved in the subsequent reactions. And the liquid phase and gases continue to react with 1 mole of Fe.

The current calculation was carried out for 1 mole of raw refractory of 47%Al_2O_3-24%SiO_2-28%C and 1 mole of Fe containing 600 ppm of Al. It was assumed that the refractory was not decarburized. When the change of reaction were infinitesimal compared with that in the previous stage, the reaction was forced to stop. In order to calculate the thickness of reacted layer, it was assumed that 1 mole of Fe was contained in a cube. The contact area between the refractory and liquid Fe was calculated to be 1.9×1.9 cm^2. The densities of Mullite, Al_2O_3, FeO–TiO_2 FeO–SiO_2–Al_2O_3(slag) were 3.52, 3.05, 4.44 and 3.0 g/cm^3, respectively. The calculation result is shown in **Fig. 12**(a). Based on Fig. 12(a), the calculation was discussed by comparing it with the experimental results. It is experimentally evident that FeO formed on Fe surface reacts with Al_2O_3–SiO_2–C refractory. FeO and SiO_2 are reduced by sufficient carbon in the refractory, resulting in the formation of Al_2O_3-enriched layer. Thus, it is likely that FeO–SiO_2–Al_2O_3 are reduced by Al in liquid Fe to generate the layer of Al_2O_3–SiO_2, which is in good agreement with some experimental results.[24–26] Another Al_2O_3 layer of 1.8 μm could originate from the reduction of SiO_2 in mullite ($3Al_2O_3 \cdot 2SiO_2$) layer by Al in liquid Fe. However, the mullite layer could be destroyed due to the unstability during cooling in actual experiments. And it is likely that Al_2O_3 inclusions were agglomerated and attached to the reacted layer, which resulted in the formation of Al_2O_3-enriched layer on the refractory observed in the current study. Therefore, it can be considered that the thermodynamic calculation show the stepwise progress of forming the first and second reacted layer.

Another calculation was carried out for 1 mole of the raw refractory of 47%Al_2O_3-24%SiO_2-28%C and 1 mole of liquid Fe containing 0.06 mass% of Al and 0.06 mass% of Ti. The other conditions are similar to those previously mentioned. The calculation results are shown in Fig. 12(b) and are compared to the experimental results by Kwon *et al*.[27] As previously explained, the Al_2O_3 layer was formed in the

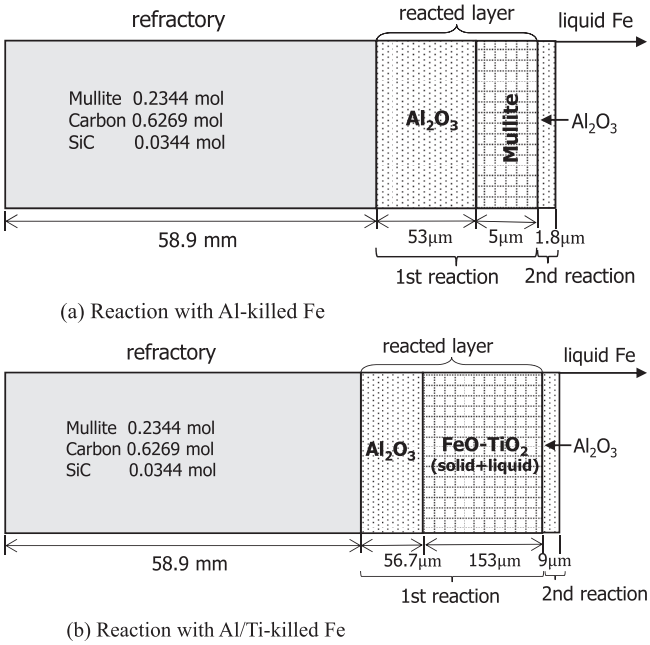

Fig. 12. Calculation results for the reaction between Al_2O_3–SiO_2–C refractory and Al-killed Fe and for that between Al_2O_3–SiO_2–C and Al/Ti-killed Fe.

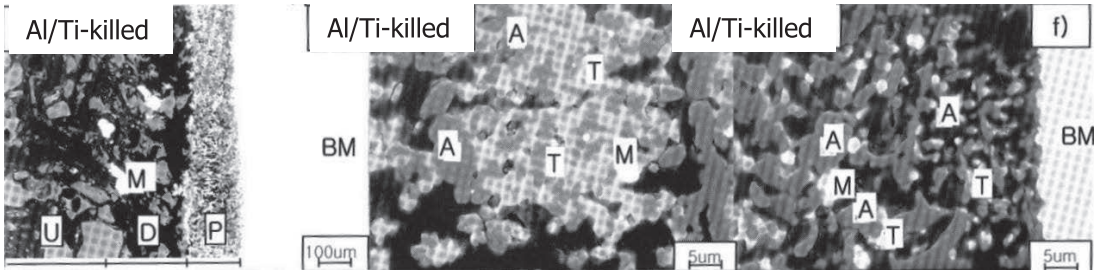

Fig. 13. Reaction between Al_2O_3–SiO_2–C refractory and Al/Ti-killed Fe. [A: Al–Ti–O, T: Ti–Al–(Fe)–O, U: unaltered layer, D: decarburized layer, P: Product layer, M: metal droplet, BM: bulk metal][27]

first reaction, and simultaneously FeO on Fe surface could combine with TiO_2 in liquid Fe to generate FeO–TiO_2 layer. However, Al_2O_3- and TiO_2-enriched inclusions are mixed together in the experimental results reported by Kwon *et al*.[27] This indicates that Al_2O_3 particles and FeO–TiO_2 inclusions mix together in the first reaction since FeO and TiO_2 exist in the solid-liquid coexisting region of the phase diagram as shown in Fig. 12(b).

4. Conclusions

The thin film method was carried out to investigate the formation mechanism of interfacial inclusions between refractory and molten steel because it has the only interfacial properties in boundary layers except for the inclusions and reactions in bulk metal. The new experimental methodology was effective in clarifying the effect of refractory materials on the interfacial reaction between Al_2O_3–SiO_2–C refractory and Al-killed/Al-Ti-killed steels. Based on the findings, the following conclusions were obtained.

(1) According to SEM/EDS analysis of the interface, when moving from the refractory side to Fe, the proportion of SiO_2 gradually decreased while the contents of FeO and Al_2O_3 increased.

(2) The reacted layer is formed in such a way that initially FeO-enriched liquid layers are widely distributed on the Fe surface and then FeO and SiO_2 in the liquid layer are reduced by Al in liquid Fe to develop solid Al_2O_3-enriched layer of inclusions.

(3) SiO_2 exposed by non-uniformity of refractory can be reacted with Al in liquid Fe, which results in forming solid Al_2O_3-enriched inclusions. This might cause the nozzle clogging.

(4) The inclusions in liquid Fe can be increased due to the oxygen remaining in Ar gas being supplied through nozzle to prevent the adherence of inclusions onto it.

(5) According to the thermodynamic calculation, the oxide layers formed at the interface are in good agreement with the experimental results previously reported for that between Al_2O_3–SiO_2–C refractory and Al-killed/Al-Ti-killed steels.

REFERENCES

1) N. Shimada: *Taikabutsu*, **28** (1976), 371.
2) I. D. Prendergast: *Iron Steelmaker*, **15** (1988), 18.
3) S. Riaz, K. C. Mills and K. Bain: *Ironmaking Steelmaking*, **29** (2002), 107.
4) G. J. Hassall, K. G. Bain, N. Jones and M. O. Warman: *Ironmaking Steelmaking*, **29** (2002), 383.
5) K. Beskow, J. Jia, C. H. P. Lupis and Du Sichen: *Ironmaking Steelmaking*, **29** (2002), 427.
6) K. Yamaguchi, S. Ogibayashi, R. Tsujino and K. Nakamura: *CAMP-ISIJ*, **3** (1990), 1216.
7) S. Ogibayashi: *Taikabutsu*, **46** (1994), 166.
8) A. Ramacciotti and E. Matino: Proc. AIME Electr. Furn. Conf., Vol. 42, Iron and Steel Society, Warrendale, Pa, (1984), 293.
9) M. Uchimura, K. Miyazawa and T. Hiromatsu: *CAMP-ISIJ*, **8** (1995), 1016.
10) N. Shinozaki, N. Echida, K. Mukai, Y. Takahashi and Y. Tanaka: *Tetsu-to-Hagané*, **80** (1994), 748.
11) R. Tsujino, A. Tanaka, A. Imamura, D. Takahashi and S. Mizoguchi: *Tetsu-to-Hagané*, **80** (1994), 765.
12) K. Sasai and Y. Mizukami: *ISIJ Int*., **34** (1994), 802.
13) T. Kaneko, T. Ono and S. Misoguchi: *Testu-to-Hagané*, **66** (1980), S868.
14) R. Dekkers, B. Blanpain, P. Wollants, F. Haers, C. Vercruyssen and B. Gommers: *Ironmaking Steelmaking*, **29** (2003), 437.
15) R. Dekkers, B. Blanpain and P. Wollants: *Metall. Mater. Trans. B*, **34B** (2003), 161.
16) Y. S. Lee, S.-M. Jung and D.-J. Min: *Ironmaking Steelmaking*, in press.
17) Slag Atlas, 2nd ed., ed. by VDEh, Verlag Stahleisen GmbH, Düsseldorf, (1995), 111.
18) H. Straube, G. Kuhnelt and E. Plockinger: *Arch. Eissenhüttenwes*., **38** (1967), 509.
19) S. W. Robinson, I. W. Martin and F. B. Pickering: *Met. Technol*., **6** (1979), 157.
20) The Japan Society for the Promotion of Science: The 19th Comm. on Steelmaking ed. by Gordon and Breach, Steelmaking Data Sourcebook, Gorden and Breech Science Publishers, New York, (1988), 45.
21) C. H. P. Lupis: Chemical Thermodynamics of Materials, Prentice Hall, New Jersey, USA, (1993), 405.
22) H. Ono-Nakazato, T. Koyama and T. Usui: *ISIJ Int*., **43** (2003), 298.
23) E. T. Turkdogan: Physical Chemistry of High Temperature Technology, London, Academic Press, (1980), 11; 81.
24) E. Kapilashrami, V. Sahajwalla and S. Seetharaman: *Ironmaking Steelmaking*, **31** (2004), 509.
25) E. Kapilashrami, V. Sahajwalla and S. Seetharaman: *ISIJ Int*., **44** (2004), 653.
26) E. Kapilashrami, A. K. Lahiri, A. W. Cramb and S. Seetharaman: *Metall. Mater. Trans. B*, **34B** (2003), 647.
27) O. D. Kwon: PhD thesis, POSTECH, (2003).